J Mol Model (2015) 21:54
DOI 10.1007/s00894-015-2603-7

ORIGINAL PAPER

Analysis of degradation mechanism of disperse orange 25 in supercritical water oxidation using molecular dynamic simulations based on the reactive force field

Jinli Zhang · Jintao Gu · You Han · Wei Li · Zhongxue Gan · Junjie Gu

Received: 20 September 2014 / Accepted: 1 February 2015

Abstract 4-[N-(2-cyanoethyl)-N-ethylamino]-4′-nitroazobenzene (disperse orange 25, DO25) is one of the main components in dyeing wastewater. In this work, supercritical water oxidation (SCWO) process of DO25 has been investigated using the molecular dynamic simulations based on the reactive force field (ReaxFF). For the SCWO system, the effects of temperature, the molecular ratio of DO25, O_2 and H_2O as well as the reaction time have been analyzed. The simulated results showed that the aromatic rings in DO25 could be attacked by hydroxyl radical, oxygen molecule, and hydroxyl radical together with oxygen molecule, respectively, which caused the aromatic ring-opening reaction to happen mainly through three different pathways. The hydroxyl radicals were mainly from water clusters and H_2O_2 (which was produced from oxygen molecules reacting with water clusters). However, for the SCW system as comparison, the aromatic rings in DO25 could be attacked by hydroxyl radical only, and the OH radicals just come from water clusters. During the DO25 SCWO degradation process, we also found that N elements in one DO25 molecule were difficult to be converted into environmentally friendly N_2 molecules because of steric hindrance, but increasing the number of DO25 molecules could improve the possibility for the connection of N elements, thus promoting N element converting into N_2. Extending reaction time could also improve N elements in DO25 to transform into N_2 rather than carbonitride.

Keywords Dyeing wastewater · Molecular dynamics · Reaction mechanism · ReaxFF · Supercritical water oxidation

Introduction

With the economic development increasing rapidly, industrial water has been consumed more and more, thus causing more wastewater discharge, which does much harm to our environment, especially for nitrogen-containing organic wastewater such as dyeing wastewater and pharmaceutical wastewater [1]. Generally, nitrogen-containing wastewater is difficult to be decomposed through biodegradable method owing to its complex components and stable structure. As an innovative technique of treating non-biodegradable wastewater, supercritical water oxidation (SCWO) proposed by Modell [2] has been widely investigated [3–6].

When the temperature and pressure reach the critical point (T_C≥374.15 °C, P_C≥22.1 MPa), water will become a kind of solvent with high diffusivity and excellent transport properties [2] and this character offers a wide field of research. For example, Bi et al. [7] investigated the pyrolysis of coal-tar asphaltene to further understand the degrading mechanism of coal-tar in SCW. A significant conclusion has been made that the conversion yield of coal-tar asphaltenein SCW was much higher than that in N_2, and it has been also used in treating wastewater [8–11]. Dyeing wastewater takes a large proportion of non-biodegradable wastewater, and its being treated by SCWO has achieved great progress. MesutAkgun et al. [10] chose DO25 as their model to study the SCWO of non-biodegradable wastewater in a tube reactor, and their results demonstrated that DO25 could be broken into water,

J. Zhang · J. Gu · Y. Han (✉) · W. Li
School of Chemical Engineering and Technology, Tianjin University, Tianjin 300072, China
e-mail: yhan@tju.edu.cn

Z. Gan
State Key Laboratory of Low Carbon Energy of Coal, ENN Group, Langfang 065001, Hebei Province, China

J. Gu
Mechanical and Aerospace Engineering, Carleton University, 1125 Colonel By Drive, Ottawa, Ontario K1S5B6, Canada

Published online: 21 February 2015

carbon dioxide, and oxynitride. Then several kinetic equations were constructed in theory, which was in accordance with their experimental data. Their kinetic equations are described as follows. The symbol *k(T)* is the reaction rate constant and X_{COD} stands for the conversion of COD. Based on the following equation, the author drew a plot between $1/T$ and $\ln k(T)$, and the figure showed the data points for the temperature dependence of the pseudo-first-order Arrhenius rate constant k, calculated for each run.

$$k(T) = \frac{-\ln(1-X_{COD})}{t}$$

Gong et al. [8] investigated the effects of pressure, temperature, and oxidant dosage ratio on the removal of chemical oxygen demand (COD) of dyeing wastewater in SCWO system and a COD removal of more than 98.4 % was achieved at 704 K and 28 MPa. Ivette Vera Pérez et al. [9] chose phenol and 2,4-dinitrophenol as models to investigate the processes of their degradation by SCWO. The results showed that both of the two models were decomposed into low molecular substances in suitable temperature, oxygen excess, and pressure. Recently, Zhang et al. [11] set up a small organic laboratory wastewater treatment plant of supercritical water oxidation. They optimized the experimental condition at the temperature of 440 °C, pressure of 26 MPa, residence time of longer than 70 s, hydrogen peroxide as oxidant with 2.6 times of excessive rate. The contents of organic pollutants and TOC met the discharge standard GB8978-1996 after their treatment process. So it can be seen that SCWO method is an effective way in treating non-biodegradable wastewater.

Although these researchers made some conclusions from their experimental phenomena, they did too little about SCWO mechanism, which is quite significant for process design and industrialization. In order to understand the SCWO mechanism of methylamine, Oshima [12] et al. proposed an elementary reaction model for the SCWO of methylamine based on a combustion mechanism that involved reactions relevant to $NH_2CH_2O_2$, and their proposed model was in good agreement with the experimental data. They gave the major reaction paths for the predicted results about the SCWO of CH_3NH_2 by their own experiments. Fujii et al. [13] investigated the roles of water as a recant in SCWO with methanol decomposed by experimental methods. They found that a reaction, $HO_2+H_2O=OH+H_2O_2$, enhanced the OH radical production and thereby facilitated the degradation of methanol. Chang et al. [14] studied the degradation of 2,4,6 –trinitrotoluene (TNT) in SCWO. By identifying TNT products using gas chromatograph-mass spectrometer-computer, they concluded that the main intermediate products of TNT degradation were linear paraffin, several dimers and directly oxidation products of TNT, such as toluene, trinitrobenzene, and dinitrotolune, and the TNT degradation reaction in SCWO was a free-radical reaction in which the free-radical generation relied on O_2 attacking C-H bond of organic molecule. Wang [15] et al. investigated SCWO of Changzhi bituminous coal and the kinetic equation they constructed matched well with the free-radical mechanism. Savage et al. [16] conducted some experiments about methane oxidation in SCW between 525 and 585 °C and at 25 MPa for residence time between 3.2 and 7.6 s in an tubular flow reactor. They concluded that OH, O_2 and HO_2 in SCW could react with methane to promote its degradation.

In the processes of nitrogen-containing organic wastewater degradation, the investigation of the migration of N element is also very important. It determines whether the N-containing products are environmentally friendly or not. Garcia-Jarana et al. [17] performed a series of experiments to find the best oxidant dosage to obtain the maximum organic conversion using N, N–dimethylformamide as a model for nitrogen-containing hydrocarbons in wastewaters. They drew a conclusion that the reaction parameters have great effects on the generation of nitrogen-containing such as NH_4^+, NO_2^-, and NO_3^-. In other studies, aminomethane was found to be converted into N_2 and N_2O after SCWO progress conducted by Benjamin and Savage [18] who have investigated the degradation of aminomethane in SCWO by experimental method. In addition, Kim et al. [19] carried out a research with an aim of a commercial plant to treat "Transformer oil contaminated with polychlorinated biphenyls (PCBs)" by a SCWO process showing that except for N_2, NO and NO_2 were identified as well.

The N-containing models that the above investigations involved are relatively simple, which could not represent the main component of dyeing wastewater. Disperse orange 25 (DO25) is short for 4-[N-(2-cyanoethyl)-N-ethylamino]-4′-nitroazobenzene. Its molecular structure (shown in Fig. 1) contains two aromatic rings, both of which are connected with a nitrogen-containing group. DO25 is a kind of dye which used for coloring plastics, and it is also the main component of non-biodegradable dyeing wastewater [20]. Therefore, DO25 was chosen in the present study to investigate the SCWO degradation mechanism of non-biodegradable dyeing wastewater using reactive molecular dynamics simulation.

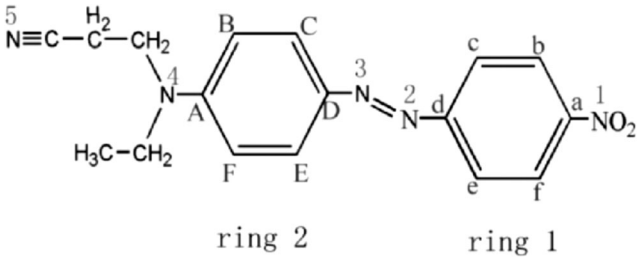

Fig. 1 The molecular structure of DO25 with serial number of benzene rings and nitrogen atoms

Our simulation results show that the generated products include CO_2, H_2O, NO_x and other intermediate products and it is consistent with Mesut Akgun's work [10]. Our theoretical work would not only be helpful for the application of SCWO technology in the field of non-biodegradable wastewater treatment, but also help facilitate the conceptual design and analysis of chemical processes based on SCW reaction media.

Computational methods

Simulation details

In our present work, a kinetic investigation of oxidation for DO25 in SCW using ReaxFF method has been carried out. ReaxFF, developed by van Duin et al. [21], is a general bond-order potential and can be used to fully address the chemistry of dynamic bonds and polarization effects. It is able to describe the evolving of formation, transition, and dissociation of chemical bonds in a molecular system when combined with molecular dynamics. Up to now, ReaxFF has been applied to combustion [22, 23], coal pyrolysis [24], and nanotube [25]. Wei et al. [26] used ReaxFF reactive force field to perform a series of molecular dynamics simulations (MDSs) on a unimolecular model compound to investigate the detailed mechanisms for lignite methanolysis. Their work illustrates that the ReaxFF reactive force field can give an atomistic description of the initial mechanism for methanolysis and provides useful insights into the complicated reaction processes. Our previous study has also investigated the coal gasification based on the Wiser model in the SCW media using ReaxFF and DFT methods [27]. From the study, we concluded that the water clusters in SCW turned into H radical-rich after providing OH radicals to the cyclic rings and it was the main source for the production of hydrogen molecules in SCW-coal system. The OH radicals were able to bind with coal intermediates to accelerate their being converted into small fragments. Besides, our previous methods and results provide effective evidence for the applicability of ReaxFF to SCW system. As a result, it is certainly reasonable for the application of ReaxFF in SCWO system.

Firstly, the DO25 structure in a three-dimensional model was optimized by the Dmol [3] module in the Materials Studio software supplied by Accelrys Inc. Partial energy analysis was also completed using the Dmol [3] module allowing us to calculate the chemical bond cracking energy. The density functional theory (DFT) calculations using Materials Studio software were at the level of the generalized gradient approximation (GGA) with the Becke–Lee–Yan–Parr (BLYP) functional employed [28]. The double numerical plus polarization (DNP) basis set was also employed here and the energy convergence criteria were set to be 0.00001 Hartree. Next, the initial structure of the reaction systems were built in accordance with the ReaxFF dynamics simulation in LAMMPS software (http://lammps.sandia.gov/). The reaction systems were constructed in periodic boxes employing the amorphous cell module. The density of pure water in supercritical state was fixed in 0.250 g/cm^3. In order to reveal the mechanism for SCWO of DO25 more clearly, another supercritical water (SCW) system without O_2 was created with the density of 0.250 g/cm^3 of pure SCW. The reaction temperature range was between 1900 and 2700 K with an interval of 200 K. Factually, researchers always choose a relatively high temperature to investigate the reaction mechanism to save simulated time based on the reactive force field. Wei's group [26] also used ReaxFF reactive molecular dynamics simulations to investigate the lignite degradation in supercritical methanol at a high temperature of 2200 K and got a good result. William A. Goddard III, the developer of ReaxFF reactive force field, has tested the effect of the different temperature scales between simulation and experiment on the thermal decomposition of brown coal, and they concluded that it may certainly affect product distributions, but the reaction processes were not affected [29]. About this illustration, our previous work [27] has demonstrated it quite clearly. So in order to make the calculation cheap, a temperature range from 1900 to 2700 K and a density of 0.250 g/cm^3 for SCW were chosen. The special simulated conditions of the two systems (SCWO and SCW) are listed in Table 1.

In the simulation, the time step was set as 0.25 fs and the NVT ensemble was applied for all the ReaxFF calculations. A multi thermostat with a damping constant of 25 ps NVT

Table 1 Simulated conditions in reaction systems

System number	System 1	System 2	System 3	System 4	System 5
DO25: O_2: H_2O	1:20:45	1:40:90	5:100:200	10:200:200	1:0:45
Density of pure (g/cm^3)	0.250	0.250	0.250	0.250	0.250
Density of system (g/cm^3)	0.547	0.497	0.584	0.919	0.350
Temperature (K)	1900–2700[a]	1900–2700	2100–2700[b]	2100–2700	1900–2700

[a] 1900–2700 stands for a series of temperatures with an interval of 200, including 1900, 2100, 2300, 2500, 2700

[b] 2100–2500 stands for a series of temperatures with an interval of 200, including 2100, 2300, 2500, 2700

calculation was used for the initial temperature from 0 to 300 K with a rising rate of 12 K/ps, then the system was equilibrated at 300 K for 2.5 ps. In order to investigate the effects of temperature on SCWO, a series of different temperature values were set and shown in Table 1. So heating up simulations were carried out from 300 K to different reaction temperatures at the rate of 40 K/ps. Next, the reactive molecular dynamics simulations were carried out for 250 and 500 ps, respectively. The calculations were repeated for three times in each of the reactive conditions and every calculation result was analyzed in detail independently.

Results and discussion

The effects of temperature and molecular ratios on SCWO

Temperature has great effects on SCWO reaction according to previous report and higher temperature contributes to more complete and higher rates of reactions [30]. In our study, 1900 K, 2100 K, 2300 K, 2500 K, and 2700 K have been chosen to explore the effects of temperature on SCWO. Because the kinetic energy stayed unchanged at the same temperature due to the NVT ensemble and the total energy is the

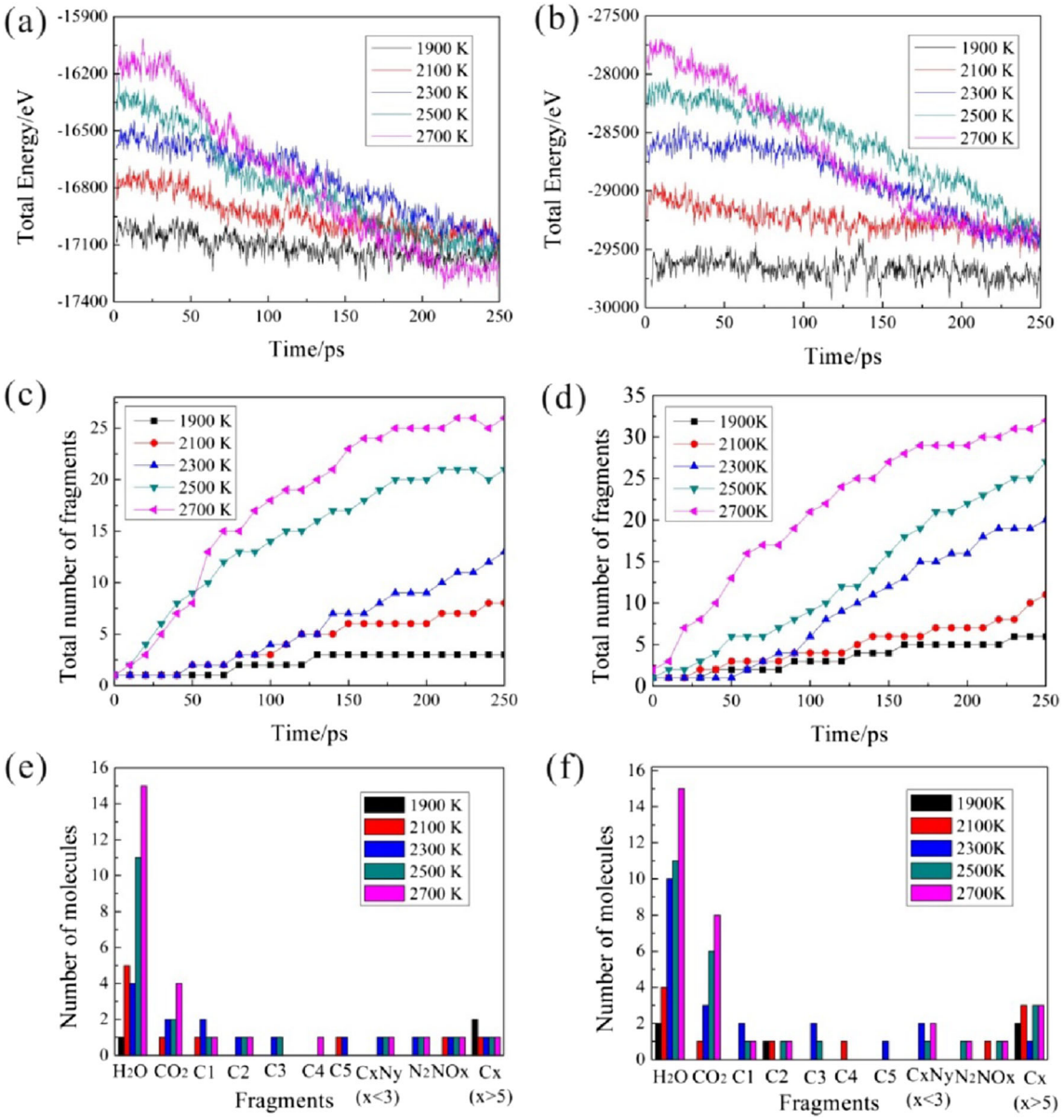

Fig. 2 The changes of total energy and total number of fragments with time in system 1 (**a**, **c**) and 2 (**b**, **d**). The final product distribution in system 1 (**e**) and system 2 (**f**). "Total energy" is the sum of potential energy and kinetic energy of the whole reaction system; "Total number of fragments" is the sum number of all the produced products and intermediates in the reaction system; "Number of molecules" is the number of produced product and intermediate respectively

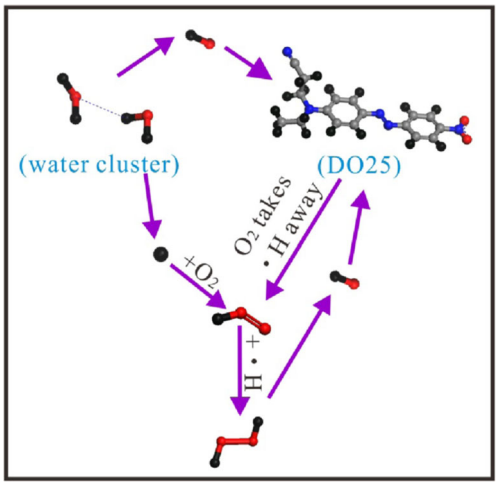

Fig. 3 The reaction paths among free radicals and molecules in SCW (●–carbon;●–oxygen;●–hydrogen;●–nitrogen)

sum of potential energy and kinetic energy, the total energy was employed to reveal the energy change of the reaction systems. The change of the total energy of the systems with the simulated time for system 1 and system 2 are shown in Fig. 2a and b. For the higher temperature (T=2700 K), the total energy stayed nearly unchanged within the first 35 ps and then began to decrease quickly. When the total number of fragments keeps nearly unchanged, we suppose the reaction to be in a stable state, and the same situation for the potential energy change. When the time reached about 210 ps, the potential energy stopped decreasing, indicating that the system was in a stable state. It was in harmony with the total number of fragments that is also unchanged at 2700 K shown in Fig. 2c and d. The trends of total energy at other temperatures were similar to the results at 2700 K except the decreasing speed is slower at lower temperature, indicating that the reaction rates were accelerated gradually with the higher temperature. Therefore, the number of the products at higher temperature is larger than that at lower temperature (shown in Fig. 2c and d). Owing to the increment of water (H_2O) and oxygen molecules (O_2) in system 2, DO25 had a greater chance to collide with them and was easier to be degraded to produce more fragments than that in system 1 at the same temperature, which led to that the total number of fragments for system 2 was larger than system 1.

Investigation of the intermediates and products is also essential to get a thorough understanding of the SCWO mechanism. Figure 2e and f showed the intermediates and product distribution at the end of 250 ps in system 1 and system 2. During the ReaxFF calculations, most of the intermediates had very short lifetime. Thus, it was difficult to be detected by the current experimental measurements. In the same reactive system, more water was generated at a higher temperature.

Table 2 The results of aromatic ring-opening reaction in system 1 within 250 ps

Temperature (K)	Times of repetition	Ring 1 opening				Ring 2 opening			
		Pathway[a]	Time[b] (ps)	Attacking position[c]		Pathway	Time (ps)	Attacking position	
				OH	O_2			OH	O_2
1900	1	OH, O_2	52.900–72.575	b	f	No ring opening			
	2	OH	8.975–30.008	c	–	OH, O_2	12.225–71.450	C	D
	3	No ring opening				O_2	198.325–205.250	–	A
2100	1	O_2	2.100–10.475	–	b	O_2	176.550–184.250	–	A
	2	OH, O_2	30.775–52.050	d	b	OH, O_2	32.500–178.200	D	B
	3	O_2	38.325–61.200	–	a	OH	91.000–187.750	D	–
2300	1	OH, O_2	69.600–116.375	d	c	OH	140.350–194.100	A	–
	2	OH, O_2	30.775–55.750	d	b	OH, O_2	48.475–178.200	C	B
	3	O_2	52.800–58.550	–	a	OH	20.125–44.875	C	–
2500	1	O_2	2.000–8.700	–	d	O_2	0–6.275	–	C
	2	OH	1.475–2.425	c	–	O_2	*	–	A
	3	Pyrolysis	24.950–25.050	–	–	OH	71.125–92.500	D	–
2700	1	O_2, OH	*[d]	c	a	OH	*	C	–
	2	OH	0.900–17.525	b	–	O_2	*	–	B
	3	OH	46.900–49.075	b	–	Pyrolysis	76.425–76.925	–	–

[a] Aromatic ring opening pathway under the action of OH, O_2 and pyrolysis

[b] The beginning and ending time of ring opening

[c] The symbol of carbon as shown in Fig. 1

[d] Aromatic rings open in the heating up process

Table 3 The results of aromatic ring-opening reaction in system 2 within 250 ps

Temperature (K)	Times of repetition	Ring 1 opening		Ring 2 opening	
		Pathway	Time (ps)	Pathway	Time (ps)
1900	1	OH, O_2	124.700–209.025	–	–
	2	–	–	O_2	51.675–74.000
	3	OH	24.225–32.875	O_2	87.650–117.625
2100	1	OH	109.575–179.175	O_2	57.550–58.500
	2	**O_2-O**	47.950–128.500	**H_2O_2**	14.300–15.675
	3	O_2	24.050–28.225	OH	181.975–213.100
2300	1	OH	60.775–89.250	OH	9.450–108.125
	2	O_2	61.800–82.500	Pyrolysis	56.875
	3	H_2O	22.825–62.475	O_2	34.650–35.425
2500	1	OH	66.725–86.800	OH, **OOH**	134.050–144.250
	2	OH	6.400–41.750	OH	21.200–22.425
	3	OH	22.850–42.250	O_2, OH	21.575–23.075
2700	1	O_2, OH	5.925–11.625	O_2	0.075–3.125
	2	OH	17.700–32.275	**H_2O**, O_2	6.075–46.250
	3	O_2, OH	6.375–13.775	Pyrolysis	50.375

Bold entries represents the attacking groups on the aromatic rings except OH radical and oxygen compared with Table 2

Among the two systems, the number of water molecules seemed to be analogous (except T=2300 K) at the same temperature. However, the quantity of the carbon dioxide in system 2 was larger than that in system 1, illustrating that the increase of oxygen was beneficial for the production of carbon dioxide. We found that there were some intermediates called C2 or C3 components at low temperature, and their structures were similar to carbon dioxide dimer or trimer. Once the temperature rose to a suitable value, these intermediates would be broken into carbon dioxide. At 2700 K, most of the H atoms from DO25 were converted into water whose hydrogen also come from SCW due to the homogeneous reaction in SCW [31, 32], and the same went for other temperatures. The detailed information of the reaction pathway will be discussed in section "Initial reaction mechanisms for oxidation of DO25 in SCW". Remarkably, the number of water at 2300 K was only 4 in system 1. Then we traced the whole reaction process and found that some of the H atoms from DO25 were transformed into OH radicals or H_2O_2. Except for H_2O and CO_2, other intermediates or products such as C3, C4 and NO_x were also observed as listed in Fig. 2e and f, although they only took a small proportion.

Initial reaction mechanisms for oxidation of DO25 in SCW

The resources of active radicals during SCWO process

In SCW, free radical reactions are supposed to take place just as previous reports stated [12, 13, 16, 33, 34]. In this work, we traced the changes of water in SCW and the oxygen molecules to clarify the reaction mechanism of SCWO. From reaction systems, three types of radicals (hydroxyl radical, hydrogen radical, and peroxyl radical) were observed in the free radical reactions. The main active radical attacking DO25 was OH radical. The Fig. 3 obtained by tracing the arc document about every reaction using the Materials Studio software showed two ways for the production of OH radicals. The first way was directly from supercritical water. The second way was more complex. Firstly, the HO_2 radical were produced through two paths: a) oxygen molecule interacted with H

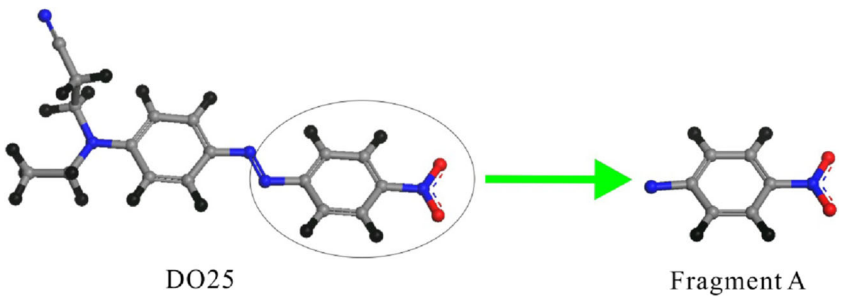

Fig. 4 3D model of disperse orange 25 and fragment A

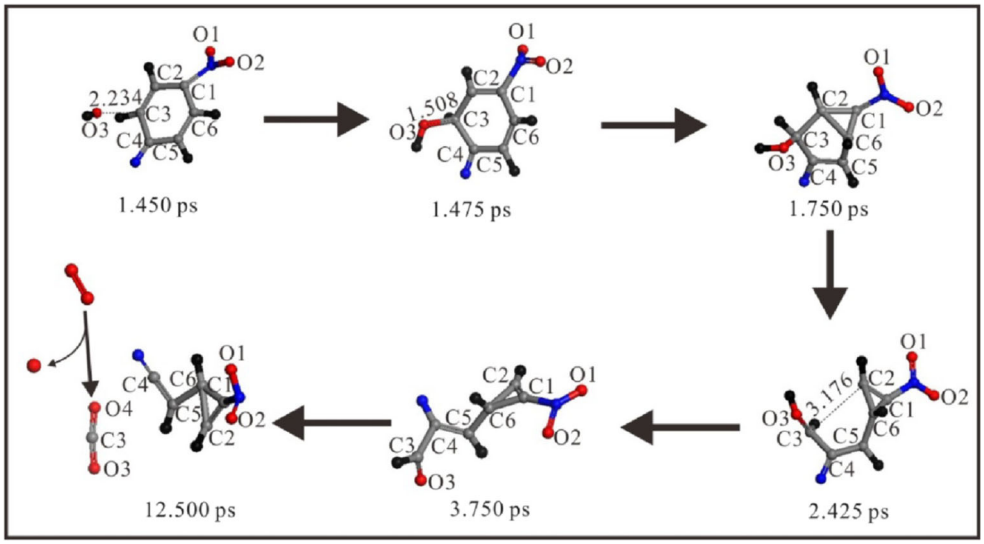

Fig. 5 The process of aromatic ring-opening reaction attacked by OH radical. This example is chosen in the second simulation at 2500 K in system 1 (The unit of the lengths is Å)

radical which was produced from water cluster to form HO_2 radical; b) oxygen molecule took a hydrogen atom away from DO25 to form HO_2 radical. Then, HO_2 radical connected with another H radical which was mainly produced from water cluster to form a H_2O_2 molecule. Finally, the H_2O_2 molecule broke into two OH radicals. Actually, DO25 can be attacked by five kinds of radicals or molecules including OH radical, O_2, HO_2 radical, H_2O_2, and H_2O in a sequence of the attacking probability from high to low. After that, these small molecular substances became part of the aromatic rings, interacting with them to accelerate ring-opening and further reactions. Not only did SCW offer a homogeneous environment, but also participated in the reaction by itself. So SCW undertook an important role in the aromatic ring-opening reaction.

H_2O_2 can produce OH radical in the SCW environment, which has also been proved in previous research [15, 16]. The OH radical is so highly reactive that it can weaken and break the chemical bonds in organics like DO25, which has been proven in our present study. Furthermore, O_2 can mix with SCW in any proportion so as to facilitate to break aromatic rings owing to its high reactivity. Besides, the O_2 molecule can also improve the aromatic ring opening. The statistic results of aromatic ring-opening for system 1 and system 2 are presented in Tables 2 and 3. In system 1, in most cases, when the temperature ranged from 1900 to 2300 K, ring 1 was broken earlier than ring 2, and ring 1 opening took less time than ring 2, while at 2500 K and 2700 K, both of the rings were open simultaneously. When the simulation temperature was below 2300 K, ring 1 and ring 2 were broken more under the attack of O_2 combined with OH radical. While above 2300 K, as the reaction that has high activation energy barrier was relatively easier to take place, the aromatic rings were much easier to be opened under the attack of a single oxygen molecule or OH radical. The aromatic ring-opening reactions even occurred in the heating up process at 2700 K. When both of the O_2 and

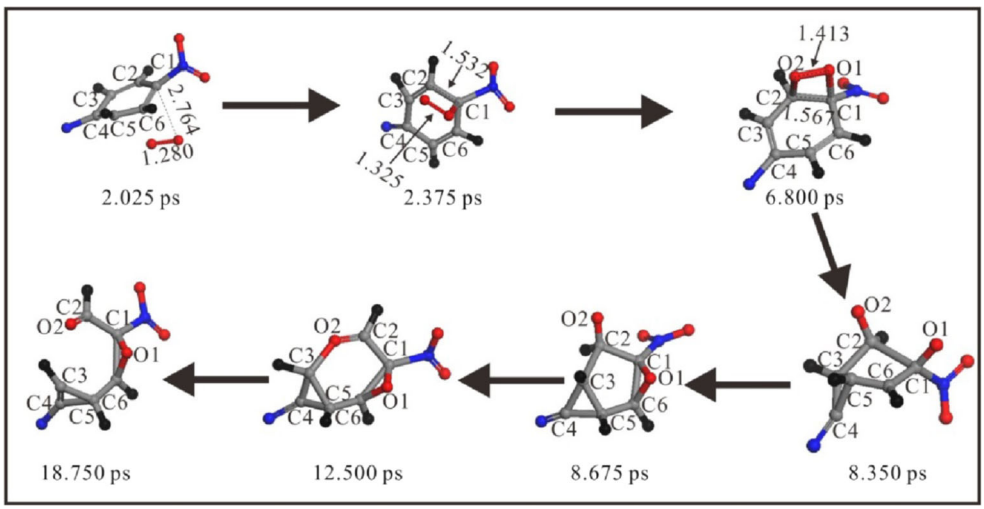

Fig. 6 The process of aromatic ring-opening reaction attacked by O_2. This example is chosen in the first simulation at 2100 K in system 1 (The unit of the lengths is Å)

OH radical acted on the aromatic rings, the attacking sequence was always hydroxyl radical followed by O_2, the reason for which is that OH radical has higher reactivity to interact with aromatic carbon than O_2. In system 2, we have found that HO_2, H_2O, and H_2O_2 were also able to attack aromatic rings except for OH radical and O_2, and all three groups left an oxygen atom on DO25 to accelerate its aromatic ring opening. However, they only took a small proportion and were not dominant.

Three pathways of aromatic ring-opening reaction during the process of SCWO and one pathway of SCW

Our simulated results showed that the aromatic rings in DO25 could be attacked by hydroxyl radical, oxygen molecule, and hydroxyl radical together with oxygen molecule, respectively, which caused the aromatic ring-opening reaction to happen mainly through three different pathways, while other paths were not predominant. In this section, fragment A (shown in Fig. 4) from the whole DO25 molecule were chosen as a representative model to conclud the three pathways for the aromatic ring-opening reaction in SCWO as shown in Figs. 5, 6, and 7.

The first pathway for the ring-opening reaction (Fig. 5) was attacked by OH radical. Initially, the OH radical was far away from ring 1, and then under the action of water clusters, it moved toward the aromatic ring. When the distance between C3 from ring 1 and O3 from OH radical turned into 1.508 Å at 1.475 ps, a chemical bond formed between them followed by structural distortion of aromatic rings. From 1.750 to 2.425 ps, the C2-C3 bond broke after OH radical attacking C3, which resulted in the opening of aromatic ring and the formation of a three-membered ring. Afterward, the OH group lost its hydrogen atom, only leaving an oxygen atom. The reaction of ring 1 only took 1 ps at 2500 K. Besides, subsequent procedures are given about ring 1 from which a C-O structure broke away to form a carbon dioxide molecule at 12.500 ps as shown in Fig. 5.

In the second pathway (Fig. 6), we found that an oxygen atom approached C1 with a changing distance from 2.764 to 1.683 Å, resulting in the formation of a chemical bond between C1 and O1. At 6.800 ps, both O1 and O2 linked to the aromatic ring, forming another bond between C2 and O2. The length of O=O bond in O_2 was increased from 1.280 to 1.325 Å as soon as O1 bond with C1, and next increased to 1.413 Å when O2 bond with C2. At 8.350 ps, the O1-O2 bond was totally broken and the aromatic ring was seriously distorted. After that, O1 moved to the bridge site of C1 and C6 at 8.675 ps, then O2 inserted into the distorted aromatic ring to bind with C2 and C3. At 18.750 ps, the distorted ring broke under the action of oxygen and SCW, and a linear chain with two three-membered rings was formed. There existed a big difference that the two oxygen atoms embed the benzene ring and participated in the formation of ringy structures compared with the former pathway (OH radical pathway). The initial step of this pathway is consistent with Chang's work [14]. They

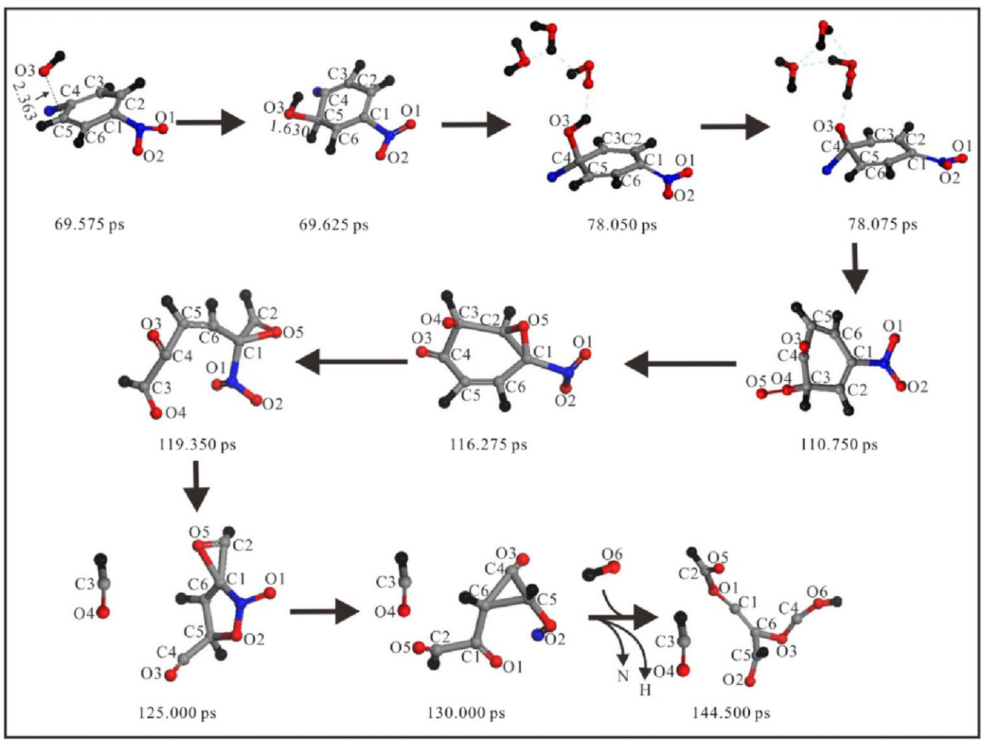

Fig. 7 The process of aromatic ring-opening reaction attacked by OH radical combined with O_2. This example is chosen in the first simulation at 2300 K in system 1 (The unit of the lengths is Å)

concluded that the TNT degradation reaction in SCWO was a free-radical reaction in which the free-radical generation relied on O_2 attacking C-H bond of organic molecule.

The third pathway for the ring-opening reaction was attacked by OH radical combined with O_2, which has been displayed in Fig. 7. In fact, it can be regarded as a combination of the first two pathways. The OH radical attacked firstly and then O_2 followed. After getting bonded with the aromatic ring, the OH group lost its hydrogen atom under the catalysis of a cluster formed by water dimer and HO_2 radical, and the hydrogen combined with the HO_2 radical to form H_2O_2 which would be broken into OH radical in the subsequent steps. Our result was consistent with previous study [16]. In their work, Savage's group [16] oxidized methane in supercritical water at 25 MPa and at temperatures between 525 and 587 °C using an isothermal, isobaric, tubular, flow reactor. One reaction route has been found by them which can be described as $H_2O_2 \rightarrow 2OH\bullet$. Our present work was consistent with Savage's work, but the combination of H radical and HO_2 was only found in our work.

(1)

$$OH + H_2O_2 = HO_2 + H_2O$$

(2)

$$OH + HO_2 = H_2O + O_2$$

(3)

$$H_2O_2 = OH + OH$$

(4)

$$HO_2 + HO_2 = O_2 + H_2O_2$$

Notably, from 69.575 to 78.050 ps, the OH group moved from C5 to C4, which can be explained as follows. The bond

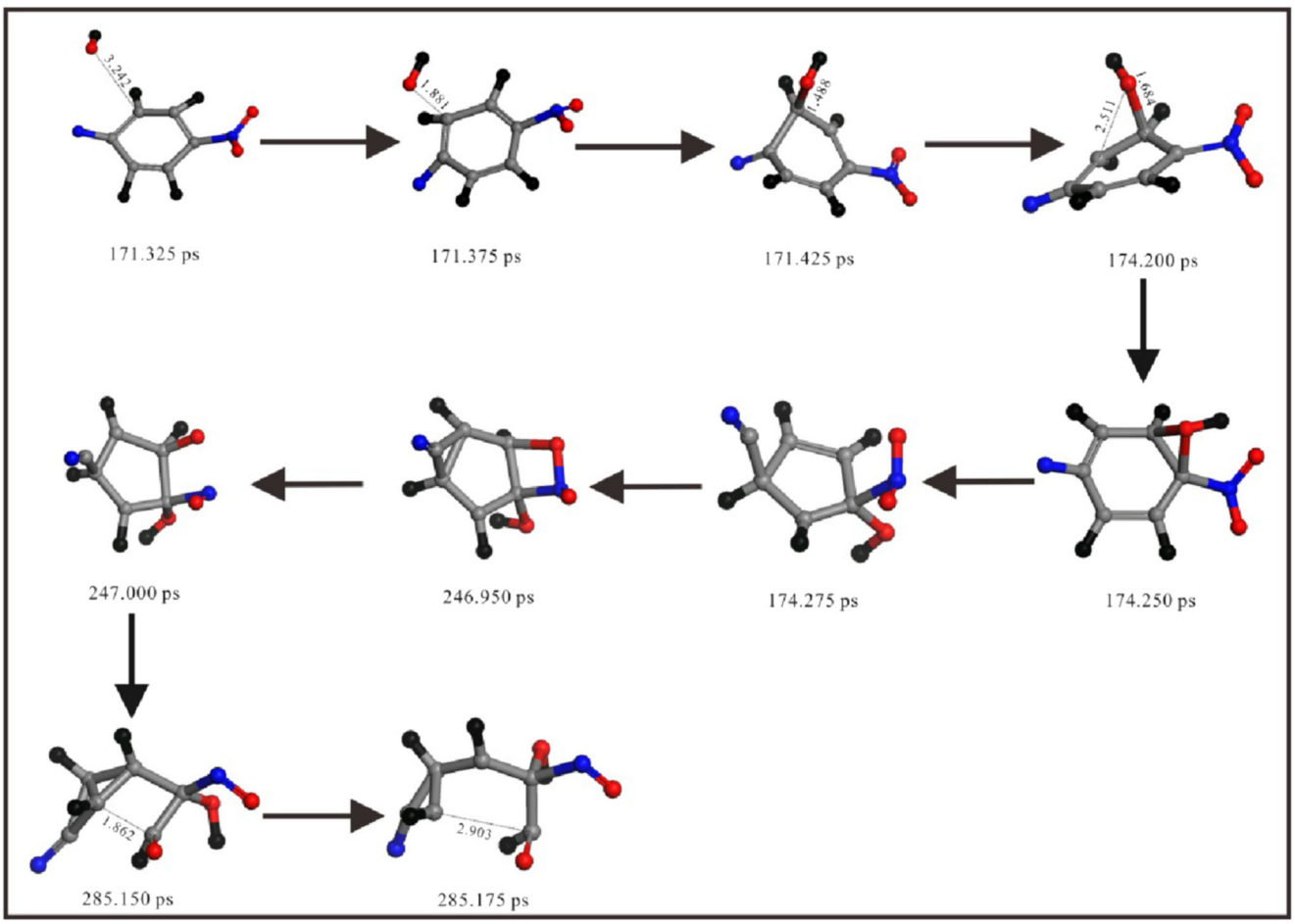

Fig. 8 The process of aromatic ring-opening reaction attacked by OH radical. This example is chosen in the first simulation at 2100 K in system 5 (The unit of the lengths is Å)

Table 4 The distribution of N-containing products in system 1 at 250 ps

Temperature (K)	Times of repetition	Products (described with molecular formula)
1900	1	No reaction took place about N
	2	No reaction took place about N
	3	No reaction took place about N
2100	1	NO_2, CHON, C_4H_3ON, $C_4H_4ON_2$
	2	N_2, NO_2, $C_9H_{12}O_4N_2$
	3	NO_2, $C_5H_3O_2N_2$, $C_{10}H_{11}O_4N_2$
2300	1	HON, C_2HON, $C_7H_6ON_3$
	2	N_2, NO_2, $C_{10}H_{10}O_2N_2$
	3	N_2, CHON, $C_5H_6ON_2$
2500	1	N_2, CHON, $C_3H_2O_2N$, $C_6H_3O_2N$
	2	CHON, CHON, C_2O_2N, HON, C_5HO_4N
	3	N_2, NO_2, $C_4H_3ON_2$
2700	1	N_2, NO, C_4HO_2N, $C_5H_3O_4N$
	2	C_2ON, C_2ON, C_2ON, C_2ON, C_3O_2N
	3	N_2, NO, $C_7O_3N_2$

strength constructed by O3 and C5 was quite weak at first, and before getting stable, it was broken by the action of water clusters probably. Next, the OH group was fixed with C4 and led to the further reaction. Next, at 110.750 ps, O_2 finished attacking and connected to C3. In the time of 116.275 ps, there were three oxygen atoms on the ringy structure totally, which contributed to accelerating the ring-opening, consequently, with the C2-C3 bond breaking down at 119.350 ps. Surprisingly, the nitrogen atom participated in the ringy structure that seldom could be seen because it was an unstable intermediate only existing for a moment. Maybe it was just one of the pathways to break into small molecules. Compared with the first two pathways, the third pathway provided more C-O bonds, thus illustrating that it was easier for the intermediates to break into small fragments because the cracking energy of C-O bond was lower than C-C bond. For example, for the structure in 144.500 ps, the cracking energy of C5-C6 bond was 318.0 kJ mol^{-1} and the C6-O3 bond was 19.7 kJ mol^{-1} via DFT method, in which case, the C6-O3 bond was very weak, while the C4-O3 bond was quite stable due to the double bond. Consequently, the C6-O3 bond was so easy to break that more small fragments would be generated.

The pathway of aromatic ring-opening in SCW has been described as well (Fig. 8). From Fig. 8, we can conclude that the process of OH radical's approaching is similar to the first pathway in SCWO. After that, the OH radical transferred from initial linking position to the carbon atom binding with nitro. At 246.950 ps, one of the oxygen atoms in $-NO_2$ bonded with neighboring carbon, and the final structure was showed in Fig. 8 at 247.000 ps. At last, under the catalysis of O and OH radical, the ring-opening reaction occurred. By tracing other SCW systems, we found that both the O atom and OH radical could promote the ring-opening by weakening C-C bond in aromatic rings.

The transformation of nitrogen element in SCWO

The migration of nitrogen is a key problem because of its huge harm to the environment. Previous studies have reported the routes of nitrogen in SCWO [18, 19], but the conclusions were variable. When Savage's group [18] studied the reaction of methylamine SCWO using a Hastelloy tubular flow reactor,

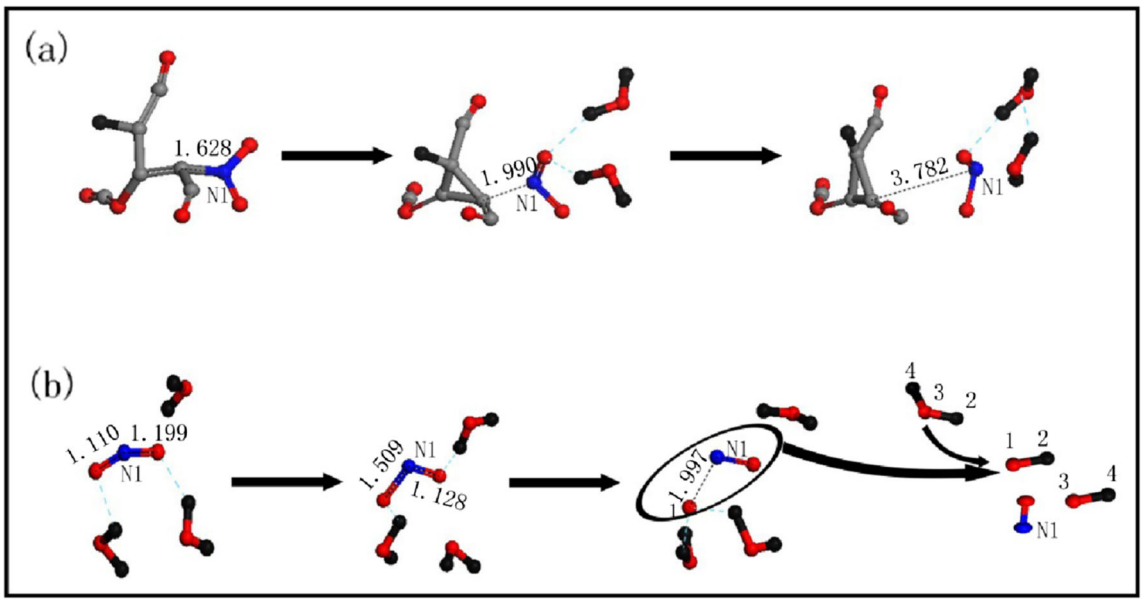

Fig. 9 The processes for the generation of NO_2 and NO in the second simulation at 2300 K in system 1 (The unit of the lengths is Å)

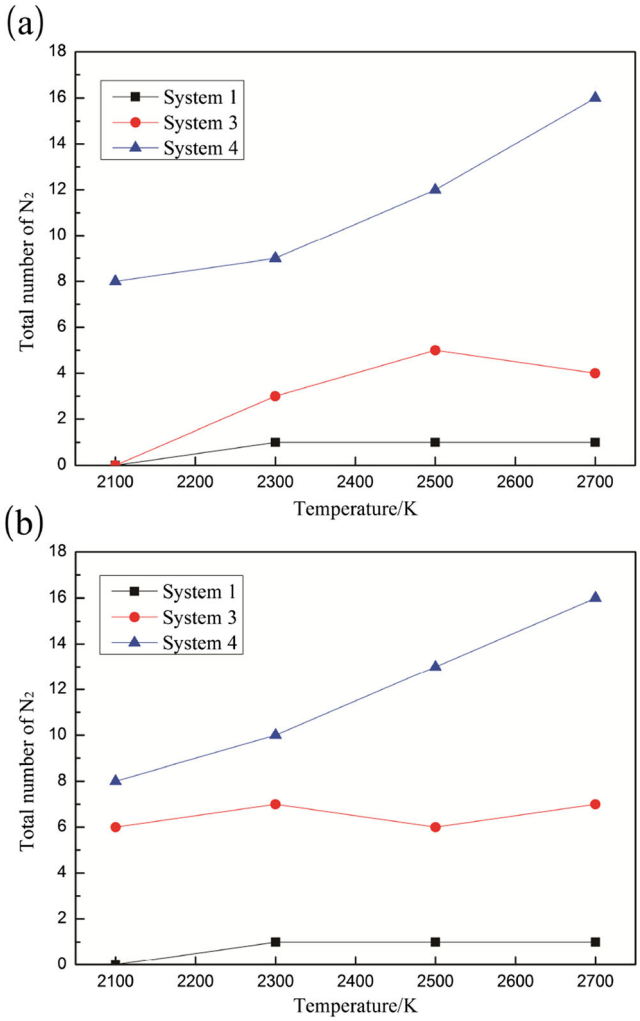

Fig. 10 Total number of N_2 at the reaction time of **a** 250 ps and **b** 500 ps under different temperatures in system 1, system 3, and system 4

they made a conclusion that the N-containing products of methylamine SCWO at 249 atm and 390–500 °C include NH_3, N_2, and N_2O. While Kim's group [19] carried out research with an aim of a commercial plant to treat transformer oil contaminated with polychlorinated biphenyls (PCBs) by a SCWO process, and their results showed that N_2, NO, and NO_2 were identified, but N_2O was not detected in their final product distribution. The results between these two articles are different, which may be due to the fact that the reaction conditions are quite different. Both of the conclusions are made from the product distribution at the end of reactions. Then we analyzed the migration routes of nitrogen element in the present study. In system 1, N_2, NO_2 and other intermediates containing the structure of C-N have been observed. Table 4 showed the product distribution in regard to N, indicating that the N-containing intermediates were smaller as the temperature got higher. In order to understand how N transformed in SCWO, the routes for N conversion were described in Fig. 9. The N1 atom in DO25 had more chances to be converted into NO_2 or NO than other N atoms due to its close interaction with oxygen atoms in $-NO_2$. It was quite easy for N2 and N3 atoms in DO25 to form a nitrogen molecule owing to their strong coaction by the double bond. However, for N4 and N5 atoms which bond with carbon atoms in the DO25 molecule structure, they were willing to be transformed into complex structures.

System 3 and system 4 were created to reveal the effects of temperature and molecular ratios on the N migration. From Fig. 10a and b, it can be seen that only N2 and N3 atoms were converted into one N_2 molecule in system 1. Because of the steric hindrance, other nitrogen atoms in DO25 were difficult to be converted into environmentally friendly N_2 molecules even when the reaction time was increased from 250 to 500 ps. When the number of DO25 molecules (system 3: ratio of $DO25/O_2/H_2O$ was 5:100:200, system 4: ratio of $DO25/O_2/H_2O$ was 10:200:200) were increased, more N_2 molecules were generated owing to the improved possibility for the connection of N atoms. Especially in system 4, when the temperature was above 2300 K, an obvious increment of nitrogen molecule appeared. It has been found that each N atom in DO25 has a chance to be converted into N_2. One example for the N_2 production through two DO25 molecules is shown in Fig. 11. During the SCWO process, the two N-containing groups from two different DO25 molecules reacted with each other gradually, and the two N atoms got together at last. Then other atoms except N broke away, only leaving a N_2 molecule finally. In system 3 and system 4, more DO25 molecules were

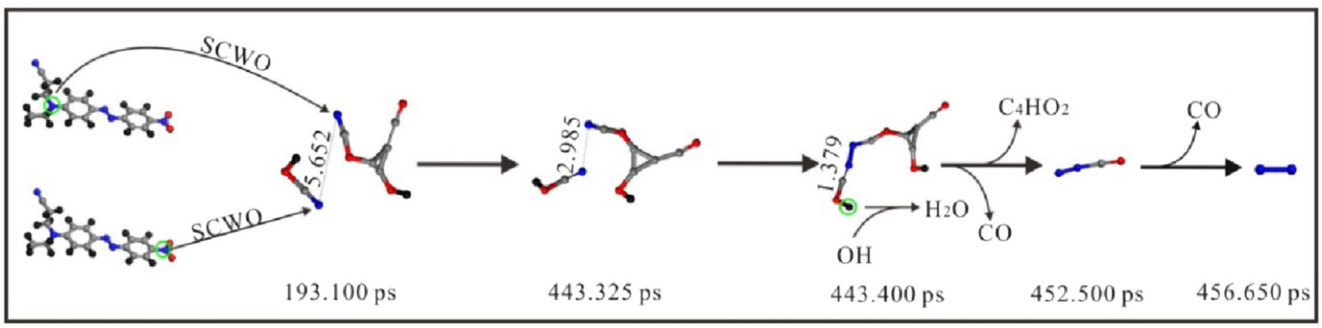

Fig. 11 The routes of N atoms in DO25. This example is chosen in the first simulation at 2300 K in system 1 at the reaction time of 500 ps (The unit of the lengths is Å)

able to generate more N-containing fragments, and they could react with each other to produce more N_2 molecules. So, extending reaction time and increasing the quantity of studied model are both helpful to obtain N_2 molecules as many as possible.

Conclusions

In order to reveal the mechanism of SCWO for DO25, ReaxFF reactive molecular simulations were carried out to investigate the effects of different temperatures, ratios of reactants in SCW system. In SCW, the free radicals and molecules including OH radical, HO_2 radical, O_2, H_2O_2, and H_2O could interact with each other and the DO25 molecule to accelerate its degradation. Especially, the key step during the degradation process of SCWO-based waste is the generation of OH radical. Its generation rate affects the degradation rate of SCWO-based waste. Three different pathways for the aromatic ring-opening reactions attacking by (a) hydroxyl radical, (b) oxygen molecule, and (c) hydroxyl radical together with oxygen molecule were concluded. A combination of OH radical and O_2 preferred to working together mostly at low temperature, while at high temperature OH radical or O_2 more probably worked alone. Besides, the N atoms could be transformed into N_2, NO_2 and other intermediates containing the structure of C-N with the simulating time of 250 ps. Extending reaction time and DO25 molecule number can also improve N elements convert into N_2 rather than carbonitride.

Acknowledgments The project was supported by the National High-Tech Research and Development Program of China (2011AA05A201), National Natural Science Foundation of China (21106094, 21206021), International Science & Technology Cooperation Program of China (2013DFG42680), the Program for Changjiang Scholars, Innovative Research Team in University (IRT1161), and Tianjin Science Foundation for Youths, China (12JCQNJC03100).

References

1. Kummerer K (2001) Drugs in the environment: emission of drugs, diagnostic aids and disinfectants into wastewater by hospitals in relation to other sources—a review. Chemosphere 45:957–969
2. Modell M (1982) Processing methods for the oxidation of organics in supercritical water. Google patents
3. Gong YM, Wang SZ, Tang XY, Xu DH, Ma HH (2014) Supercritical water oxidation of acrylic acid production wastewater. Environ Technol 35:907–916
4. Marrone PA (2013) Supercritical water oxidation-current status of full-scale commercial activity for waste destruction. J Supercrit Fluids 79:283–288
5. Shin YH, Lee HS, Veriansyah B, Kim J, Kim DS, Lee HW, Youn YS, Lee YW (2012) Simultaneous carbon capture and nitrogen removal during supercritical water oxidation. J Supercrit Fluids 72:120–124
6. Wang Q, Lv YK, Zhang R, Jicheng BI (2013) Treatment of cotton printing and dyeing wastewater by supercritical water oxidation. Desalin Water Treat 51:7025–7035
7. Han LN, Zhang R, Bi JC, Cheng LM (2011) Pyrolysis of coal-tar asphaltene in supercritical water. J Anal Appl Pyrolysis 91:281–287
8. Gong WJ, Li F, Xi DL (2008) Oxidation of industrial dyeing wastewater by supercritical water oxidation in transpiring-wall reactor. Water Environ Res 80:186–192
9. Perez IV, Rogak S, Branion R (2004) Supercritical water oxidation of phenol and 2,4-dinitrophenol. J Supercrit Fluids 30:71–87
10. Sogut OO, Akgun M (2007) Treatment of textile wastewater by SCWO in a tube reactor. J Supercrit Fluids 43:106–111
11. Dong X, Wang Y, Li X, Yu Y, Zhang M (2014) Process simulation of laboratory wastewater treatment via supercritical water oxidation. Ind Eng Chem Res 53:7723–7729
12. Li H, Oshima Y (2005) Elementary reaction mechanism of methylamine oxidation in supercritical water. Ind Eng Chem Res 44:8756–8764
13. Fujii T, Hayashi R, Kawasaki S, Suzuki A, Oshima Y (2011) Water density effects on methanol oxidation in supercritical water at high pressure up to 100 MPa. J Supercrit Fluids 58:142–149
14. Chang SJ, Liu YC (2007) Degradation mechanism of 2,4,6-trinitrotoluene in supercritical water oxidation. J Environ Sci 19:1430–1435
15. Wang SZ, Guo Y, Wang LA, Wang YZ, Xu DH, Ma HH (2011) Supercritical water oxidation of coal: investigation of operating parameters' effects, reaction kinetics and mechanism. Fuel Process Technol 92:291–297
16. Savage PE, Yu JL, Stylski N, Brock EE (1998) Kinetics and mechanism of methane oxidation in supercritical water. J Supercrit Fluids 12:141–153
17. Garcia-Jarana MB, Kings I, Sanchez-Oneto J, Portela JR, Al-Duri B (2013) Supercritical water oxidation of nitrogen compounds with multi-injection of oxygen. J Supercrit Fluids 80:23–29
18. Benjamin KM, Savage PE (2005) Supercritical water oxidation of methylamine. Ind Eng Chem Res 44:5318–5324
19. Kim K, Son SH, Kim K, Kim K, Kim YC (2010) Environmental effects of supercritical water oxidation (SCWO) process for treating transformer oil contaminated with polychlorinated biphenyls (PCBs). Chem Eng J 165:170–174
20. Ngo TT, Liotta CL, Eckert CA, Kazarian SG (2003) Supercritical fluid impregnation of different Azo-dyes into polymer: in situ Uv/Vis spectroscopic study. J Supercrit Fluids 27:215–221
21. van Duin ACT, Dasgupta S, Lorant F, Goddard WA (2001) ReaxFF: a reactive force field for hydrocarbons. J Phys Chem A 105:9396–9409
22. Chenoweth K, van Duin ACT, Dasgupta S, Goddard WA (2009) Initiation mechanisms and kinetics of pyrolysis and combustion of JP-10 hydrocarbon jet fuel. J Phys Chem A 113:1740–1746
23. Chenoweth K, van Duin ACT, Goddard WA (2008) ReaxFF reactive force field for molecular dynamics simulations of hydrocarbon oxidation. J Phys Chem A 112:1040–1053
24. Salmon E, Behar F, Lorant F, Hatcher PG, Marquaire PM (2009) Early maturation processes in coal. Part 1: pyrolysis mass balance and structural evolution of coalified wood from the morwell brown coal seam. Org Geochem 40:500–509
25. Nielson KD, van Duin ACT, Oxgaard J, Deng WQ, Goddard WA (2005) Development of the ReaxFF reactive force field for describing transition metal catalyzed reactions, with application to the initial stages of the catalytic formation of carbon nanotubes. J Phys Chem A 109:493–499
26. Chen B, Wei XY, Yang ZS, Liu C, Fan X, Qing Y, Zong ZM (2012) ReaxFF reactive force field for molecular dynamics simulations of lignite depolymerization in supercritical methanol with lignite-related model compounds. Energy Fuel 26:984–989
27. Zhang JL, Weng XX, Han Y, Li W, Cheng JY, Gan ZX, Gu JJ (2012) The effect of supercritical water on coal pyrolysis and

hydrogen production: a combined ReaxFF and DFT study. Fuel 108:682–690
28. Lee C, Yang W, Parr RG (1988) Development of the Colle–Salvetti correlation-energy formula into a functional of the electron density. Phys Rev B 37:785–789
29. Salmon E, van Duin ACT, Lorant F, Marquaire PM, Goddard WA III (2009) Early maturation processes in coal. Part 2: reactive dynamics simulations using the ReaxFF reactive force field on morwell brown coal structures. Org Geochem 40:1195–1209
30. Jin FM, Kishita A, Moriya T, Enomoto H (2001) Kinetics of oxidation of food wastes with H_2O_2 in supercritical water. J Supercrit Fluids 19:251–262
31. Bermejo MD, Cocero MJ (2006) Supercritical water oxidation: a technical review. AIChE J 52:3933–3951
32. Koda S, Maeda K, Sugimoto K, Sugiyama M (2006) Oxidation reactions of solid carbon in supercritical water. Combust Sci Technol 178:487–507
33. Koda S, Kanno N, Fujiwara H (2001) Kinetics of supercritical water oxidation of methanol studied in a CSTR by means of Raman spectroscopy. Ind Eng Chem Res 40:3861–3868
34. Phenix BD, Dinaro JL, Tatang MA, Tester JW, Howard JB, McRae GJ (1998) Incorporation of parametric uncertainty into complex kinetic mechanisms: application to hydrogen oxidation in supercritical water. Combust Flame 112:132–146